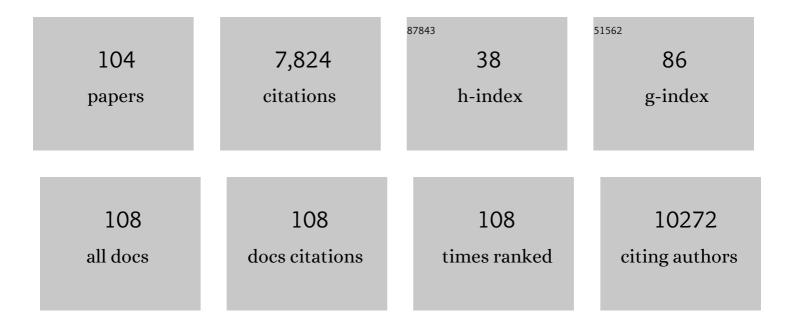
List of Publications by Year in descending order

Source: https://exaly.com/author-pdf/4584257/publications.pdf Version: 2024-02-01



#	Article	IF	CITATIONS
1	Microglia emerge from erythromyeloid precursors via Pu.1- and Irf8-dependent pathways. Nature Neuroscience, 2013, 16, 273-280.	7.1	1,121

 $_{2}$ S100 proteins in mouse and man: from evolution to function and pathology (including an update of) Tj ETQq0 0 0 rgBT /Overlock 10 Tf

3	A multimodal RACE-specific inhibitor reduces amyloid β–mediated brain disorder in a mouse model of Alzheimer disease. Journal of Clinical Investigation, 2012, 122, 1377-1392.	3.9	507
4	Binding of S100 proteins to RAGE: An update. Biochimica Et Biophysica Acta - Molecular Cell Research, 2009, 1793, 993-1007.	1.9	413
5	RAGE regulation and signaling in inflammation and beyond. Journal of Leukocyte Biology, 2013, 94, 55-68.	1.5	336
6	S100 proteins structure functions and pathology. Frontiers in Bioscience - Landmark, 2002, 7, d1356-1368.	3.0	327
7	Molecular basis for manganese sequestration by calprotectin and roles in the innate immune response to invading bacterial pathogens. Proceedings of the National Academy of Sciences of the United States of America, 2013, 110, 3841-3846.	3.3	325
8	RAGE: a single receptor fits multiple ligands. Trends in Biochemical Sciences, 2011, 36, 625-632.	3.7	267
9	S100B and S100A6 Differentially Modulate Cell Survival by Interacting with Distinct RAGE (Receptor) Tj ETQq1 1 2007, 282, 31317-31331.	0.784314 1.6	rgBT /Ove 234
10	Structural and functional insights into RAGE activation by multimeric S100B. EMBO Journal, 2007, 26, 3868-3878.	3.5	219
11	Structural Basis for Ligand Recognition and Activation of RAGE. Structure, 2010, 18, 1342-1352.	1.6	195
12	<scp>USP</scp> 18 lack in microglia causes destructive interferonopathy of the mouse brain. EMBO Journal, 2015, 34, 1612-1629.	3.5	178
13	The Extracellular Region of the Receptor for Advanced Glycation End Products Is Composed of Two Independent Structural Unitsâ€. Biochemistry, 2007, 46, 6957-6970.	1.2	156
14	Mutations in POGLUT1, Encoding Protein O-Glucosyltransferase 1, Cause Autosomal-Dominant Dowling-Degos Disease. American Journal of Human Genetics, 2014, 94, 135-143.	2.6	136
15	Cryo-EM structure of a transthyretin-derived amyloid fibril from a patient with hereditary ATTR amyloidosis. Nature Communications, 2019, 10, 5008.	5.8	127
16	Cryo-EM structure of a light chain-derived amyloid fibril from a patient with systemic AL amyloidosis. Nature Communications, 2019, 10, 1103.	5.8	120
17	Natural and amyloid selfâ€essembly of S100 proteins: structural basis of functional diversity. FEBS Journal, 2010, 277, 4578-4590.	2.2	115
18	The Receptor for Advanced Glycation End-Products (RAGE) Is Only Present in Mammals, and Belongs to a Family of Cell Adhesion Molecules (CAMs). PLoS ONE, 2014, 9, e86903.	1.1	115

#	Article	IF	CITATIONS
19	Structure of the V. cholerae Na+-pumping NADH:quinone oxidoreductase. Nature, 2014, 516, 62-67.	13.7	107
20	The Presence of an Iron-Sulfur Cluster in Adenosine 5′-Phosphosulfate Reductase Separates Organisms Utilizing Adenosine 5′-Phosphosulfate and Phosphoadenosine 5′-Phosphosulfate for Sulfate Assimilation. Journal of Biological Chemistry, 2002, 277, 21786-21791.	1.6	96
21	HMGB1 conveys immunosuppressive characteristics on regulatory and conventional T cells. International Immunology, 2012, 24, 485-494.	1.8	85
22	Structural basis of the specificity of USP18 toward ISG15. Nature Structural and Molecular Biology, 2017, 24, 270-278.	3.6	85
23	Structure of adenylylsulfate reductase from the hyperthermophilic Archaeoglobus fulgidus at 1.6-A resolution. Proceedings of the National Academy of Sciences of the United States of America, 2002, 99, 1836-1841.	3.3	78
24	Formin mDia1 Mediates Vascular Remodeling via Integration of Oxidative and Signal Transduction Pathways. Circulation Research, 2012, 110, 1279-1293.	2.0	78
25	Plant Adenosine 5′-Phosphosulfate Reductase Is a Novel Iron-Sulfur Protein. Journal of Biological Chemistry, 2001, 276, 42881-42886.	1.6	77
26	Alzheimer β-Amyloid Homodimers Facilitate Aβ Fibrillization and the Generation of Conformational Antibodies. Journal of Biological Chemistry, 2003, 278, 35317-35324.	1.6	64
27	USP18 – a multifunctional component in the interferon response. Bioscience Reports, 2018, 38, .	1.1	61
28	NADH Oxidation by the Na+-translocating NADH:Quinone Oxidoreductase from Vibrio cholerae. Journal of Biological Chemistry, 2004, 279, 21349-21355.	1.6	51
29	The Crystal Structure of Metal-free Human EF-hand Protein S100A3 at 1.7-Ã Resolution. Journal of Biological Chemistry, 2002, 277, 33092-33098.	1.6	50
30	Implications on zinc binding to S100A2. Biochimica Et Biophysica Acta - Molecular Cell Research, 2007, 1773, 457-470.	1.9	49
31	The neuronal S100B protein is a calcium-tuned suppressor of amyloid-β aggregation. Science Advances, 2018, 4, eaaq1702.	4.7	49
32	Electron spin relaxation of copper(II) complexes in glassy solution between 10 and 120K. Journal of Magnetic Resonance, 2006, 179, 92-104.	1.2	48
33	Molecular characterization of ubiquitinâ€specific protease 18 reveals substrate specificity for interferonâ€stimulated gene 15. FEBS Journal, 2014, 281, 1918-1928.	2.2	48
34	Adenylylsulfate reductases from archaea and bacteria are 1:1 αβ-heterodimeric iron-sulfur flavoenzymes - high similarity of molecular properties emphasizes their central role in sulfur metabolism. FEBS Letters, 2000, 473, 63-66.	1.3	47
35	The Function of the [4Fe-4S] Clusters and FAD in Bacterial and Archaeal Adenylylsulfate Reductases. Journal of Biological Chemistry, 2002, 277, 26066-26073.	1.6	47
36	V domain of RAGE interacts with AGEs on prostate carcinoma cells. Prostate, 2008, 68, 748-758.	1.2	45

#	Article	IF	CITATIONS
37	The crystal structures of human S100B in the zinc- and calcium-loaded state at three pH values reveal zinc ligand swapping. Biochimica Et Biophysica Acta - Molecular Cell Research, 2011, 1813, 1083-1091.	1.9	43
38	Probing the structure of the human Ca2+- and Zn2+-binding protein S100A3: spectroscopic investigations of its transition metal ion complexes, and three-dimensional structural model. Biochimica Et Biophysica Acta - Molecular Cell Research, 1998, 1448, 264-276.	1.9	38
39	Reaction Mechanism of the Ironâ^'Sulfur Flavoenzyme Adenosine-5â€~-Phosphosulfate Reductase Based on the Structural Characterization of Different Enzymatic Statesâ€,‡. Biochemistry, 2006, 45, 2960-2967.	1.2	38
40	Quinone Reduction by the Na + -Translocating NADH Dehydrogenase Promotes Extracellular Superoxide Production in Vibrio cholerae. Journal of Bacteriology, 2007, 189, 3902-3908.	1.0	37
41	Localization and Function of the Membrane-bound Riboflavin in the Na+-translocating NADH:Quinone Oxidoreductase (Na+-NQR) from Vibrio cholerae. Journal of Biological Chemistry, 2010, 285, 27088-27099.	1.6	36
42	S100A6 Amyloid Fibril Formation Is Calcium-modulated and Enhances Superoxide Dismutase-1 (SOD1) Aggregation. Journal of Biological Chemistry, 2012, 287, 42233-42242.	1.6	36
43	Pattern Recognition with a Fibril-Specific Antibody Fragment Reveals the Surface Variability of Natural Amyloid Fibrils. Journal of Molecular Biology, 2011, 408, 529-540.	2.0	34
44	Vibrio natriegens as Host for Expression of Multisubunit Membrane Protein Complexes. Frontiers in Microbiology, 2018, 9, 2537.	1.5	33
45	Expression and purification of the soluble isoform of human receptor for advanced glycation end products (sRAGE) from Pichia pastoris. Biochemical and Biophysical Research Communications, 2006, 347, 4-11.	1.0	31
46	Crystal Structure of Ca2+-Free S100A2 at 1.6-Ã Resolution. Journal of Molecular Biology, 2008, 378, 933-942.	2.0	30
47	Metal ions modulate the folding and stability of the tumor suppressor protein S100A2. FEBS Journal, 2009, 276, 1776-1786.	2.2	29
48	Central role of the Na+-translocating NADH:quinone oxidoreductase (Na+-NQR) in sodium bioenergetics of Vibrio cholerae. Biological Chemistry, 2014, 395, 1389-1399.	1.2	29
49	Receptor for advanced glycation end products: a key molecule in the genesis of chronic kidney disease vascular calcification and a potential modulator of sodium phosphate co-transporter PIT-1 expression. Nephrology Dialysis Transplantation, 2019, 34, 2018-2030.	0.4	28
50	Three-Dimensional Structure of the Nonaheme CytochromecfromDesulfovibrio desulfuricansEssex in the Fe(III) State at 1.89 à Resolutionâ€,‡. Biochemistry, 2001, 40, 1308-1316.	1.2	27
51	Nonaheme Cytochromec, a New Physiological Electron Acceptor for [Ni,Fe] Hydrogenase in the Sulfate-Reducing BacteriumDesulfovibrio desulfuricansEssex:Â Primary Sequence, Molecular Parameters, and Redox Propertiesâ€. Biochemistry, 2001, 40, 1317-1324.	1.2	27
52	Spectroscopic investigation and determination of reactivity and structure of the tetraheme cytochromec3fromDesulfovibrio desulfuricansEssex 6. FEBS Journal, 2001, 268, 3028-3035.	0.2	27
53	The structure of Na+-translocating of NADH:ubiquinone oxidoreductase of Vibrio cholerae: implications on coupling between electron transfer and Na+ transport. Biological Chemistry, 2015, 396, 1015-1030.	1.2	27
54	Oxidant-induced formation of a neutral flavosemiquinone in the Na+-translocating NADH:Quinone oxidoreductase (Na+-NQR) from Vibrio cholerae. Biochimica Et Biophysica Acta - Bioenergetics, 2008, 1777, 696-702.	0.5	26

#	Article	IF	CITATIONS
55	Conserving energy with sulfate around 100 °C – structure and mechanism of key metal enzymes in hyperthermophilic Archaeoglobus fulgidus. Metallomics, 2013, 5, 302.	1.0	26
56	Pathogenicity of POFUT1 in Dowling-Degos Disease: Additional Mutations and Clinical Overlap with Reticulate Acropigmentation of Kitamura. Journal of Investigative Dermatology, 2015, 135, 615-618.	0.3	25
57	Analysis of S100 Oligomers and Amyloids. Methods in Molecular Biology, 2012, 849, 373-386.	0.4	23
58	Intrinsically Disordered and Aggregation Prone Regions Underlie Î ² -Aggregation in S100 Proteins. PLoS ONE, 2013, 8, e76629.	1.1	22
59	The Catalytic Redox Activity of Prion Protein–Cu ^{II} is Controlled by Metal Exchange with the Zn ^{II} –Thiolate Clusters of Zn ₇ Metallothioneinâ€3. ChemBioChem, 2012, 13, 1261-1265.	1.3	18
60	How USP 18 deals with ISG 15â€modified proteins: structural basis for the specificity of the protease. FEBS Journal, 2018, 285, 1024-1029.	2.2	17
61	Metal-free MIRAS phasing: structure of apo-S100A3. Acta Crystallographica Section D: Biological Crystallography, 2002, 58, 1255-1261.	2.5	16
62	Purification, crystallization and preliminary X-ray diffraction studies on human Ca2+-binding protein S100B. Acta Crystallographica Section F: Structural Biology Communications, 2005, 61, 673-675.	0.7	16
63	Crystallization of the Na+-translocating NADH:quinone oxidoreductase fromVibrio cholerae. Acta Crystallographica Section F: Structural Biology Communications, 2010, 66, 1677-1679.	0.7	16
64	A capture method based on the VC1 domain reveals new binding properties of the human receptor for advanced glycation end products (RAGE). Redox Biology, 2017, 11, 275-285.	3.9	16
65	Altered Notch Signaling in Dowling-Degos Disease: Additional Mutations in POGLUT1 and Further Insights into Disease Pathogenesis. Journal of Investigative Dermatology, 2019, 139, 960-964.	0.3	15
66	High yield expression of catalytically active USP18 (UBP43) using a Trigger Factor fusion system. BMC Biotechnology, 2012, 12, 56.	1.7	14
67	Crystallization and preliminary analysis of the NqrA and NqrC subunits of the Na+-translocating NADH:ubiquinone oxidoreductase fromVibrio cholerae. Acta Crystallographica Section F, Structural Biology Communications, 2014, 70, 987-992.	0.4	13
68	Crystallization of the NADH-oxidizing domain of the Na+-translocating NADH:ubiquinone oxidoreductase fromVibrio cholerae. Acta Crystallographica Section F: Structural Biology Communications, 2006, 62, 110-112.	0.7	11
69	Identification of a novel mutation in <i>RIPK4</i> in a kindred with phenotypic features of Bartsocasâ€Papas and CHAND syndromes. American Journal of Medical Genetics, Part A, 2015, 167, 2555-2562.	0.7	11
70	Fast fragment- and compound-screening pipeline at the Swiss Light Source. Acta Crystallographica Section D: Structural Biology, 2022, 78, 328-336.	1.1	11
71	A Sodium-Translocating Module Linking Succinate Production to Formation of Membrane Potential in Prevotella bryantii. Applied and Environmental Microbiology, 2021, 87, e0121121.	1.4	10
72	Dynamic interactions and Ca2+-binding modulate the holdase-type chaperone activity of S100B preventing tau aggregation and seeding. Nature Communications, 2021, 12, 6292.	5.8	10

#	Article	IF	CITATIONS
73	The structure of Ca ²⁺ â€loaded S100A2 at 1.3â€Ã resolution. FEBS Journal, 2012, 279, 1799-1810.	. 2.2	9
74	Strong pH dependence of coupling efficiency of the Na ⁺ – translocating NADH:quinone oxidoreductase (Na ⁺ -NQR) of <i>Vibrio cholerae</i> . Biological Chemistry, 2017, 398, 251-260.	1.2	9
75	An improved expression system for the VC1 ligand binding domain of the receptor for advanced glycation end products in Pichia pastoris. Protein Expression and Purification, 2015, 114, 48-57.	0.6	8
76	Generation and characterization of a novel, permanently active S100P mutant. Biochimica Et Biophysica Acta - Molecular Cell Research, 2009, 1793, 1078-1085.	1.9	7
77	Inactivation of the Na+-translocating NADH:ubiquinone oxidoreductase fromVibrio alginolyticusby reactive oxygen species. FEBS Journal, 2002, 269, 1287-1292.	0.2	6
78	Purification and crystallization of the human EF-hand tumour suppressor protein S100A2. Acta Crystallographica Section F: Structural Biology Communications, 2006, 62, 1120-1123.	0.7	6
79	Expression and purification of neurolin immunoglobulin domain 2 from Carrassius auratus (goldfish) in Escherichia coli. Protein Expression and Purification, 2008, 59, 47-54.	0.6	6
80	Crystallization and calcium/sulfur SAD phasing of the human EF-hand protein S100A2. Acta Crystallographica Section F: Structural Biology Communications, 2010, 66, 1032-1036.	0.7	6
81	Cu ²⁺ -binding to S100B triggers polymerization of disulfide cross-linked tetramers with enhanced chaperone activity against amyloid-l² aggregation. Chemical Communications, 2021, 57, 379-382.	2.2	6
82	The Mouse-Specific Splice Variant mRAGE_v4 Encodes a Membrane-Bound RAGE That Is Resistant to Shedding and Does Not Contribute to the Production of Soluble RAGE. PLoS ONE, 2016, 11, e0153832.	1.1	6
83	Crystallization and preliminary X-ray analysis of adenylylsulfate reductase fromArchaeoglobus fulgidus. Acta Crystallographica Section D: Biological Crystallography, 2000, 56, 1673-1675.	2.5	5
84	The Na+-translocating NADH:quinone oxidoreductase (Na+-NQR) from Vibrio cholerae enhances insertion of FeS in overproduced NqrF subunit. Journal of Inorganic Biochemistry, 2008, 102, 1366-1372.	1.5	5
85	Sulfate to go. Science, 2015, 350, 1476-1477.	6.0	5
86	Respiratory Membrane Protein Complexes Convert Chemical Energy. Sub-Cellular Biochemistry, 2019, 92, 301-335.	1.0	5
87	Prothrombin is a binding partner of the human receptor of advanced glycation end products. Journal of Biological Chemistry, 2020, 295, 12498-12511.	1.6	5
88	Receptor for Advanced Glycation End Products is Involved in Platelet Hyperactivation and Arterial Thrombosis during Chronic Kidney Disease. Thrombosis and Haemostasis, 2020, 120, 1300-1312.	1.8	5
89	Central Carbon Metabolism, Sodium-Motive Electron Transfer, and Ammonium Formation by the Vaginal Pathogen Prevotella bivia. International Journal of Molecular Sciences, 2021, 22, 11925.	1.8	5
90	Low-resolution structure determination of Na+-translocating NADH:ubiquinone oxidoreductase fromVibrio choleraebyab initiophasing and electron microscopy. Acta Crystallographica Section D: Biological Crystallography, 2012, 68, 724-731.	2.5	4

#	Article	IF	CITATIONS
91	Structural Heterogeneity and Bioimaging of S100 Amyloid Assemblies. , 2014, , 197-212.		4
92	Impact of Na ⁺ -Translocating NADH:Quinone Oxidoreductase on Iron Uptake and <i>nqrM</i> Expression in Vibrio cholerae. Journal of Bacteriology, 2020, 202, .	1.0	4
93	The Family of S100 Cell Signaling Proteins. , 2003, , 87-93.		4
94	The deletion of amino acids 114–121 in the TM1 domain of mouse prion protein stabilizes its conformation but does not affect the overall structure. Biochimica Et Biophysica Acta - Molecular Cell Research, 2008, 1783, 1076-1084.	1.9	3
95	The Family of S100 Cell Signaling Proteins. , 2010, , 983-993.		3
96	Sodium as Coupling Cation in Respiratory Energy Conversion. Metal Ions in Life Sciences, 2016, 16, 349-390.	2.8	3
97	Anoxic cell rupture of Prevotella bryantii by high-pressure homogenization protects the Na+-translocating NADH:quinone oxidoreductase from oxidative damage. Archives of Microbiology, 2020, 202, 1263-1266.	1.0	3
98	X-ray Structural Analysis of S100 Proteins. Methods in Molecular Biology, 2013, 963, 87-97.	0.4	3
99	S4.28 Crystal structure of the NADH-oxidizing FAD domain from the Na+-translocating NADH:quinone oxidoreductase (Na+-NQR). Biochimica Et Biophysica Acta - Bioenergetics, 2008, 1777, S39.	0.5	2
100	Concise Synthesis of 1,4â€Benzoquinoneâ€Based Natural Products as Mitochondrial Complex I Substrates and Substrateâ€Based Inhibitors. ChemMedChem, 2020, 15, 2491-2499.	1.6	2
101	AgeR deletion decreases soluble fms-like tyrosine kinase 1 production and improves post-ischemic angiogenesis in uremic mice. Angiogenesis, 2021, 24, 47-55.	3.7	1
102	Living on Sulfate: Three-Dimensional Structure and Spectroscopy of Adenosine 5´-Phosphosulfate Reductase and Dissimilatory Sulfite Reductase. , 2008, , 13-23.		1
103	1H, 13C, and 15N resonance assignments of the second immunoglobulin domain of neurolin from Carassius auratus. Biomolecular NMR Assignments, 2013, 7, 65-67.	0.4	0
104	A miniaturized assay for kinetic characterization of the Na+-translocating NADH:ubiquinone oxidoreductase from Vibrio cholerae. Analytical Biochemistry, 2017, 537, 56-59.	1.1	0